

---

# Class Distribution Shifts in Zero-Shot Learning: Learning Robust Representations

---

Yuli Slavutsky

Department of Statistics and Data Science  
The Hebrew University of Jerusalem

Yuval Benjamini

Department of Statistics and Data Science  
The Hebrew University of Jerusalem

## Abstract

Distribution shifts between training and deployment data often affect the performance of machine learning models. In this paper, we explore a setting where a hidden variable induces a shift in the distribution of classes. These distribution shifts are particularly challenging for zero-shot classifiers, as they rely on representations learned from training classes, but are deployed on new, unseen ones. We introduce an algorithm to learn data representations that are robust to such class distribution shifts in zero-shot verification tasks. We show that our approach, which combines hierarchical data sampling with out-of-distribution generalization techniques, improves generalization to diverse class distributions in both simulations and real-world datasets.

## 1 INTRODUCTION

Few-shot learning (Fei-Fei et al., 2006) addresses classification with limited training data, where only a few examples from each class are available. A special case is zero-shot learning (Larochelle et al., 2008), where the classifier is used in deployment on new classes that were unseen during training. To allow for the *open-world* classification, zero-shot classifiers are often modeled as verification algorithms: they determine whether a given pair of data points belong to the same class or not. For instance, in person re-identification (Hermans et al., 2017b) the task is to identify whether two data points (e.g., face images or voice recordings) belong to the same person.

Many popular verification techniques are based on *deep metric learning* (for reviews see Roth et al. (2020); Musgrave et al. (2020)). These methods

train deep neural networks to map data-points to a representation space, where examples from the same class are close in some given distance function, whereas those from different classes are farther apart. Common deep metric learning approaches include contrastive-learning (Hadsell et al., 2006), siamese neural networks (Koch et al., 2015), triplet networks (Hoffer and Ailon, 2015), and more recent variations (Oh Song et al., 2016; Sohn, 2016; Wu et al., 2017; Yuan et al., 2019). Most zero-shot methods based on these approaches rely on the assumption that the classes seen in training and those used in deployment come from the same distribution. This assumption is implicitly incorporated into the design of test sets (Xian et al., 2019; Gu et al., 2020), and is explicitly used to assess the ability of zero-shot classifiers to generalize (Zheng et al., 2018; Slavutsky and Benjamini, 2021). However, in real-life applications, training classes are often chosen based on convenience and accessibility considerations during the data collection. Even with careful collection, the distribution of classes might shift over the course of deployment.

Class distribution shifts have been extensively studied in the general setting of supervised learning. In *Class-Imbalanced Learning* (Lin et al., 2017; Cui et al., 2019; Cao et al., 2019) it is assumed that some classes are more dominant in training, while in deployment this is no longer the case. Therefore, solutions classically include data or loss re-weighting (Shimodaira, 2000; Byrd and Lipton, 2019; Ren et al., 2020; Menon et al., 2020) and calibration of the classification score (Saerens et al., 2002; Zhong et al., 2021). A particularly popular framework is *Distributionally Robust Optimization* (DRO) (Ben-Tal et al., 2013; Duchi et al., 2021; Duchi and Namkoong, 2021; Wei et al., 2023), where instead of assuming a specific probability distribution, a set or a range of possible distributions is considered, and optimization is performed to achieve best results over the worst-case distribution. A special case known as *Group DRO* (Sagawa et al., 2019; Piratla et al., 2021), involves a group variable that introduces discriminatory patterns

among classes within specific groups. This framework includes methods that assume that the classifier does not have access to the group information, and therefore propose re-weighting high loss examples (Liu et al., 2021), and data sub-sampling to balance classes and groups (Idrissi et al., 2022). However, in all these examples it is assumed that classification is performed in a *closed-world* setting. That is, they rely on the evaluation class set being identical to the training one.

Class distribution shifts are particularly challenging for zero-shot verification classifiers, which depend on a representation learned from the training classes to distinguish new, unseen ones. Typically, these classifiers are trained using Empirical Risk Minimization (ERM) to achieve good separation among the training classes. However, representations learned via ERM might perform poorly on distributions that substantially deviate from the class distribution in the training data. Notably, in person re-identification, this concern gained attention from a fairness perspective with respect to gender bias (Grother et al., 2019; Klare et al., 2012), age bias (Best-Rowden and Jain, 2017; Michalski et al., 2018; Srinivas et al., 2019) and racial bias (Raji and Buolamwini, 2019; Wang et al., 2019). Note that in all these examples it is known which variable (i.e., gender, age, race) is expected to cause the distribution shift.

However, in real-world scenarios, the attribute responsible for the class distribution shift is often unknown during training, thus causing a particular challenge. In such cases, approaches based on collecting balanced datasets or re-weighting training examples (Wang et al., 2019; Robinson et al., 2020; Wang and Deng, 2020) are inapplicable, and novel methods need to be developed.

In this paper we address this challenge and make three key contributions: (i) we introduce a simple model to investigate class distribution shifts in zero-shot learning, which provides insights into why ERM might fail in such situations. (ii) We present a framework for constructing artificial data “environments” using hierarchical sub-sampling, which enables adaptation of existing methods from the field of out-of-distribution (OOD) generalization (Peters et al., 2016; Arjovsky et al., 2019) to enhance robustness of zero-shot classifiers against class distribution shifts. (iii) We propose a new balancing term that can be incorporated as a regularization component within our framework. This term is particularly well-suited for zero-shot verification algorithms trained using deep metric learning losses.

We introduce the motivating model in Section 2.

Existing OOD methods are discussed in Section 3, and our proposed approach is presented in Section 4. We evaluate our method through simulation studies in Section 5.1 and demonstrate its enhanced robustness on real-world datasets in Section 5.2.

### 1.1 Preliminaries and Notation

Let  $\{z_i, c_i\}_{i=1}^{N_z}$  be a labeled set of training data points  $z \in \mathcal{Z}$  and classes  $c \in \mathcal{C}$ , such that  $c_i$  is the class of  $z_i$ . We assume that each class  $c$  is characterized by some attribute  $A$ , and that the training classes are sampled according to

$$P_C(c) = \int P_{C|A}(c|a)P_A(a) da. \quad (1)$$

However, the mixture of the attribute  $A$  differs from training to evaluation and therefore the evaluation classes are sampled according to

$$Q_C(c) = \int P_{C|A}(c|a)Q_A(a) da. \quad (2)$$

We assume that the variable  $A$  is unknown, and that both in training and evaluation, data points  $z \in \mathcal{Z}$  for each class are sampled according to  $P_{Z|C}(z|c)$ .

We focus on verification algorithms that determine whether a pair of data-points  $x_{ij} := (z_i, z_j)$  belong to the same class. We denote this by  $y_{ij}$ , where  $y_{ij} = 1$  if  $c_i = c_j$  and  $y_{ij} = 0$  otherwise. When the identity of each data point in the pair is not important, we use a single index for simplicity, namely  $(x_m, y_m)$ .

Our goal is to learn a representation function  $g : \mathcal{Z} \rightarrow \hat{\mathcal{Z}}$  such that in the representation space  $\hat{\mathcal{Z}}$ , data points of the same class are closer than those from different classes, according to a predefined distance function  $d$ .

To assess the quality of the representation we treat distances between representations  $d_g(z_i, z_j) := d(g(z_i), g(z_j))$  as classification scores. Following common practice in the field (see, for example, Sixta et al. (2020); Joshi et al. (2022)), we use the area under the receiver operating characteristic curve (AUC) to evaluate the representation, allowing for threshold-agnostic assessment:

$$AUC(g) := P(d_g(z_i, z_j) < d_g(z_u, z_v) | y_{ij} = 1, y_{uv} = 0). \quad (3)$$

We assume that  $g$  is a neural network and that it is trained by optimizing a deep-metric-learning loss, such as the contrastive loss:

$$\begin{aligned} \ell(z_i, z_j, y_{ij}; d_g) := & y_{ij}d_g(z_i, z_j) \\ & + (1 - y_{ij}) \max\{0, m - d_g(z_i, z_j)\}, \end{aligned} \quad (4)$$

where  $m \geq 0$  is a margin defining the limit distance between data-points from different classes. Note that for  $m = 0$  the loss is reduced to the first term and is not affected by negative examples.

## 2 A SIMPLE MODEL OF CLASS DISTRIBUTION SHIFTS

**Data distribution:** Assume that for all classes the data points  $z_i \in \mathbb{R}^d$  are sampled from a Gaussian distribution, centered around their class mean  $c_i$ , all with the same covariance matrix  $\Sigma_z$ . That is,  $z_i|c_i \sim \mathcal{N}(c_i, \Sigma_z)$ , where  $\Sigma_z = \nu_z \cdot I_d$ , and  $I_d$  is the identity matrix.

**Class distribution:** Let an attribute  $A$  be a variable indicating the type to which a class  $c$  belongs, and assume there are two types:  $a_1$  and  $a_2$ . The classes  $c_i$  are drawn according to a Gaussian distribution  $c_i \sim \mathcal{N}(0, \Sigma_a)$  for  $a \in \{a_1, a_2\}$ , where  $\Sigma_a$  is a diagonal matrix with replicates of three distinct values on its diagonal:  $\nu_0, \nu^+, \nu^-$ . Let  $0 < \nu^- < \nu_z < \nu_0 < \nu^+$ . That is, in the coordinates corresponding to  $\nu_0$  and  $\nu^+$  data points from different classes can be relatively well separated, whereas in the coordinates corresponding to  $\nu^-$  they are not.

Assume that the coordinates corresponding to  $\nu_0$  are the same for both types, but  $\nu^+$  and  $\nu^-$  are swapped:

$$\begin{aligned} \Sigma_{a_1} &= \text{diag}(\nu_0, \dots, \nu_0, \nu^+, \dots, \nu^+, \nu^-, \dots, \nu^-) \\ \Sigma_{a_2} &= \text{diag}(\nu_0, \dots, \nu_0, \nu^-, \dots, \nu^-, \nu^+, \dots, \nu^+) \end{aligned}$$

An illustration of this model with one replicate of each value is shown in Figure 1.

Assume that  $P(a_1) = \rho$  where  $\rho \gg 0.5$ , while  $Q(a_1) = 1 - \rho$ . That is, the majority of classes in training are of type  $a_1$ , while during evaluation the majority is of type  $a_2$ .

**Representation:** For simplicity, assume that the representation is given by  $g(z) = wz$ , where  $w \in \{0, 1\}^d$  is a binary such that  $\sum_{n=1}^d w_n = k < d$ . In essence, this representation corresponds to selecting  $k$  dimensions (coordinates) of the input  $z$  (i.e., feature selection).

**ERM solution:** Since  $\nu_z < \nu_0$ , choosing the dimensions corresponding to  $\nu_0$  will achieve relatively good separation between classes of both types, but even better separation will be achieved on the dimensions corresponding to  $\nu^+$ . Therefore, ERM is prone to choose the dimensions corresponding to  $\nu^+$  for classes in  $a_1$ , which will lead to poor performance during deployment, since in these dimensions the classes of type  $a_2$  correspond to  $\nu^-$  and therefore are not well separated.

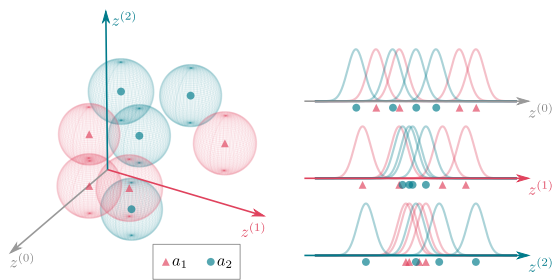


Figure 1: Illustration of the Model. Data points  $z$  are depicted in three dimensions. Classes of type  $a_1$  and  $a_2$  are represented with red triangles and green circles correspondingly. Left: Three-dimensional spheres represent regions where 95% of the data points in each Gaussian distribution lie. Right: PDF curves corresponding to the projection of each class in each coordinate. Classes of type  $a_1$  (red) are best separated in  $z^{(1)}$  (red axis), where classes of type  $a_2$  (green) are clustered there together. Conversely, classes of type  $a_2$  are well separated in  $z^{(2)}$  (green axis), where classes of type  $a_1$  are not. In  $z^{(0)}$  (grey axis) classes of both types can be separated, but not as effectively as on their respective optimal axes.

**Robustness:** In this model a robust approach entails selecting the shared dimensions, offering relatively good separation for both class types, despite distribution shifts.

## 3 BACKGROUND ON OOD GENERALIZATION

The field of OOD generalization considers a setting where the assumption that training data and classes are sampled from the same joint distribution  $P_{C,Z}(c, z) = P_{Z|C}(z|c)P_C(c)$  both at training and evaluation time, is violated. Instead it is assumed that it changes across different environments (Meinshausen and Bühlmann, 2015; Rothenhäusler et al., 2021).

This field gained attention since the work of Peters et al. (2016) and Peters et al. (2017) which defined invariance of a prediction to different environments within a causal framework. These works were followed by Arjovsky et al. (2019), who presented the first approach compatible with deep learning, called *Invariant Risk Minimization* (IRM). Since then, several approaches that rely on access to diverse training environments were proposed to recover the features responsible for the casual relationship between a data point  $z$  and its class  $c$ . Those include choosing causal variables using statistical tests (Rojas-Carulla et al., 2018), leveraging the conditional independences

induced by the common causal mechanism (Chang et al., 2020), and using multi-domain calibration as a trainable surrogate for OOD performance (Wald et al., 2021).

Most relevant to our work are methods that consider the representation  $g = g_\theta$  as a neural network parametrized by  $\theta$ , and optimize an objective of the form

$$\min_{\theta} \sum_{e \in E_{\text{train}}} \ell^e(g_\theta) + \lambda R(g_\theta, E_{\text{train}}) \quad (5)$$

where  $\ell^e(g_\theta)$  is the empirical loss obtained on the environment  $e$ ,  $E_{\text{train}}$  is the set of all training environments,  $R$  is a regularization term over multiple environments, and  $\lambda$  is a regularization factor balancing between the ERM term and the invariance penalty. We present below three such methods, which we refer to in the next sections of this paper.

**Invariant Risk Minimization (IRM)** (Arjovsky et al., 2019) aims to find data representations  $g_\theta$  such that the optimal classifier  $w$  on top of that data representation  $w \circ g_\theta$ , is the same for all environments:

$$\begin{aligned} \min_{\theta} \quad & \sum_{e \in E_{\text{train}}} \ell^e(w \circ g_\theta) \\ \text{s.t } w \in \quad & \arg \min_{w'} \ell^e(w' \circ g_\theta) \quad \forall e \in E_{\text{train}}. \end{aligned} \quad (6)$$

However, since this objective is too hard to optimize, the authors propose a relaxed objective:

$$\min_{\theta} \sum_{e \in E_{\text{train}}} \ell^e(g_\theta) + \lambda \sum_{e \in E_{\text{train}}} R_{\text{IRMv1}}^e(g_\theta), \quad (7)$$

where

$$R_{\text{IRMv1}}^e(g_\theta) = \|\nabla_{w|w=1} \ell^e(w \cdot g_\theta)\|^2 \quad (8)$$

measures how close  $w$  is to minimizing  $\ell^e(w \circ g_\theta)$ .

Note that for loss functions, for which optimal classifiers can be written as conditional expectations, the original IRM objective is equivalent to the requirement that for all  $e, e' \in E_{\text{train}}$

$$\mathbb{E}_{P_{C,Z}^e} [c|g(z) = h] = \mathbb{E}_{P_{C,Z}^{e'}} [c|g(z) = h]. \quad (9)$$

where  $P_{C,Z}^e$  and  $P_{C,Z}^{e'}$  are the joint data distribution in environments  $e$  and  $e'$  respectively.

**Calibration Loss Over Environments (CLOvE)** (Wald et al., 2021) leverages the equivalence in Equation 9 to establish a link between multi-environment calibration and invariance for binary predictors ( $c \in \{0, 1\}$ ). The authors then propose a regularizer based on *Maximum Mean Calibration Error* (MMCE) (Kumar et al., 2018) which uses

universal kernels to measure the expected calibration error on a single environment. Let  $f : \hat{Z} \rightarrow [0, 1]$  be a classification score function applied on the representation  $f \circ g$ , and  $f_i = \max\{f \circ g(z_i), 1 - f \circ g(z_i)\}$  be the *confidence* on the  $i$ -th data point. Denote by  $b_i = \mathbb{1}\{|c_i - f_i| < \frac{1}{2}\}$  the *correctness*, and let  $K : \mathbb{R} \times \mathbb{R} \rightarrow \mathbb{R}$  be a universal kernel. Then the MMCE is given by

$$\begin{aligned} R_{\text{MMCE}}^e(f, g_\theta) = & \quad (10) \\ & \frac{1}{m^2} \sum_{z_i, z_j \in Z^e} (b_i - f_i)(b_j - f_j) K(f_i, f_j) \end{aligned}$$

where  $Z^e$  corresponds to training data points in the environment  $e$ . The authors propose the objective

$$\min_{\theta} \sum_{e \in E_{\text{train}}} \ell^e(g_\theta) + \lambda \sum_{e \in E_{\text{train}}} R_{\text{MMCE}}^e(f, g_\theta). \quad (11)$$

However, the equivalence between OOD generalization and calibration was shown only for linear models in an infinite population. Therefore, while showing encouraging results in practice, enforcing calibration does not guarantee achieving OOD generalization on finite environment sets or with non-linear models.

**Variance Risk Extrapolation (VarREx)** proposed by Krueger et al. (2021), is based on the observation that reducing differences in loss (risk) across training domains can reduce a model's sensitivity to a wide range of distributional shifts. The authors found that using the variance of losses as a regularizer is stabler and more effective compared to other penalties. Therefore, they propose the following objective:

$$\min_{\theta} \sum_{e \in E_{\text{train}}} \ell^e(g_\theta) + \lambda R_{\text{VarREx}}(g_\theta, E_{\text{train}}) \quad (12)$$

$$R_{\text{VarREx}}(g_\theta, E_{\text{train}}) = \text{Var}(\ell^{e_1}(g_\theta), \dots, \ell^{e_n}(g_\theta)) \quad (13)$$

where  $n$  is the number of training environments.

While simple and intuitive, this approach assumes that losses on different environments accurately reflect the classifier's performance on those environments. However, as discussed in the next section, this is often not the case for deep metric learning losses.

Note that all the aforementioned approaches assume closed-world classification, and that the training data arrives from several *labeled* environments. Similarly to other studies on distribution shift, this assumption implies that training data includes explicit information regarding the potential sources of the shift.

## 4 PROPOSED APPROACH

In this section, we present a new algorithm, designed to learn representations for zero-shot verification

classifiers, that are robust to class distribution shifts. We assume these shifts stem from changes in an unknown (hidden) attribute variable  $A$  associated with each class.

Our approach revolves around two key ideas: (i) during training, different mixtures of the attribute  $A$  can be achieved in small subsets of the classes, and (ii) ensuring strong performance across diverse mixtures increases the robustness of the representation to the mixture encountered at deployment time.

### 4.1 Synthetic Environments

Standard ERM training involves sampling pairs of data points  $(z_i, a_j)$  uniformly at random from all classes available during training. However, as discussed in Section 2, this procedure is susceptible to overfitting to the attribute mixture in training. Note that if the attribute causing the class distribution shift were known, different mixtures could be created, and treated as distinct environments. Then, existing OOD methods could be used to ensure generalization across these mixtures.

Let  $N_c$  be the number of classes available during training. While class subsets of similar size to  $N_c$  maintain attribute distributions similar to the overall training set, subsets comprising of only  $k$  classes with  $k \ll N_c$  are likely to showcase distinct attribute distributions. Therefore, we tackle the attribute being unknown by hierarchically sampling data pairs: first, sample a subset of  $k$  classes,  $S = \{c_1, \dots, c_k\}$ . Then, for each  $c \in S$  sample  $2r$  pairs of data points as follows:  $r$  pairs from within the class  $c$ ,  $\{z_i; c_i = c\}$ , uniformly at random (positive pairs); and  $r$  negative pairs, where one point is uniformly at random from  $c$ , and the other from all other data points in  $S$ ,  $\{z_i; c_i \neq c, c_i \in S\}$ . Here for simplicity we create balanced environments, but different proportions of positive examples can be considered instead.

This hierarchical sampling allows us to naturally achieve diverse attribute mixtures, and we consider such mixtures  $\mathcal{S} = \{S_1, \dots, S_n\}$  as synthetic environments.

**The Number of Synthetic Environments**  
 OOD generalization techniques typically involve optimization over all environments simultaneously. However, given our consideration of small subsets of classes and a large  $N_c$ , the number of possible subsets,  $\binom{N_c}{k}$  is substantial. For computational reasons, we propose sampling  $n \ll \binom{N_c}{k}$  subsets  $S$  at each training iteration. To allow generalization to an attribute  $a$  that is associated with at least  $\rho \in (0, 1)$  of the training classes, an appropriate size of  $n$  needs to be set. We

propose choosing  $n$  such that with high probability of  $(1 - \alpha)$ , the  $n$  class subsets  $S_1, \dots, S_n$  would include at least one subset with at least two classes associated with  $a$  (otherwise none of the subsets would contain negative pairs with the attribute  $a$ ).

Denote the probability of a given subset to not contain neither class associated with  $a$  by  $\phi_0 = \binom{\binom{1-\rho}{k} N_c}{\binom{N_c}{k}}$ , and the probability of a given subset to contain exactly one such class by  $\phi_1 = \rho N_c \binom{\binom{1-\rho}{k-1} N_c}{\binom{N_c}{k}}$ . Then this corresponds to setting  $n$  to

$$n \approx \frac{\log(\alpha)}{\log(\phi_0 + \phi_1)}. \quad (14)$$

### 4.2 Balancing Term

While any of the OOD penalties discussed in Section 3 can be used to balance performance across the synthetic environments, we propose using the variance of AUC values as a penalty.

Denote the set of negative pairs by  $D_l^0 = \{x_{ij} = (z_i, z_j) : c_i, c_j \in S_l, y_{ij} = 0\}$ , and the set of positive pairs by  $D_l^1 = \{x_{ij} = (z_i, z_j) : c_i, c_j \in S_l, y_{ij} = 1\}$ . An unbiased estimator of the AUC on a given class subset  $S_l$  is given by

$$\widetilde{\text{AUC}}(S_l, g; d) = \frac{1}{|D_l^0| |D_l^1|} \sum_{x_{ij} \in D_l^1} \sum_{x_{uv} \in D_l^0} \mathbb{1}[d_g(x_{ij}) < d_g(x_{uv})] \quad (15)$$

However, this estimator is non-differentiable, and therefore cannot be used as a penalty in gradient-descent based optimization. Instead, we use an approximation named *soft-AUC* (Calders and Jaroszewicz, 2007), where the step function is approximated with a steep sigmoid:

$$\widehat{\text{AUC}}(S_l, g; d) = \frac{1}{|D_l^0| |D_l^1|} \sum_{x_{ij} \in D_l^1} \sum_{x_{uv} \in D_l^0} \text{sigmoid}_\beta(d_g(x_{uv}) - d_g(x_{ij})), \quad (16)$$

where  $\text{sigmoid}_\beta(t) = \frac{1}{1+e^{-\beta t}}$ . Note that when  $\beta \rightarrow \infty$ ,  $\text{sigmoid}_\beta$  converges pointwise to the step function.

Consequently, we propose optimizing the penalized objective

$$\min_{\theta} \sum_{l=1}^n \ell^{S_l}(g_\theta) + \lambda R_{\text{VarAUC}}(S_1, \dots, S_n) \quad (17)$$

where

$$R_{\text{VarAUC}}(S_1, \dots, S_n) = \widehat{\text{Var}}\left(\widehat{\text{AUC}}(S_1, g; d), \dots, \widehat{\text{AUC}}(S_n, g; d)\right). \quad (18)$$

We outline our combined approach in Algorithm 1. For notation simplicity we assume the unpenalized training loss is applied to pairs of data points  $(x_{ij}, y_{ij}) = ((z_i, z_j), \mathbb{1}_{c_i=c_j})$ , but it can be easily adapted for any tuple size (for example triplets). Note that our algorithm can also be easily adapted to other regularization penalties instead of VarAUC.

**Remark:** Our proposed penalty, like VarREx, aims to reduce differences across attribute distributions, enhancing robustness to various shifts. However, unlike VarREx, we propose to measure the performance directly instead of relying on the loss, which, in deep metric learning algorithms, is distance-based. The reason behind this is the fact that in zero-shot verification algorithms, the sampled tuples often contain numerous easy negative examples, causing performance to plateau quickly, whereas the distances themselves may vary considerably. Sampling strategies such as selection of the most difficult tuples (Hermans et al., 2017a) were proposed to address this. However, those methods have been found to produce noisy gradients and loss values (Musgrave et al., 2020). In contrast, the AUC evaluates the classifier’s ability to rank positive examples higher than negative ones, regardless of the scale of representation distances, making it potentially less noisy with respect to easy negative examples.

**Justified Minimization of Variance on Subsets**

Denote by  $N_s = \binom{N_c}{k}$  the number of all possible subsets of  $k$  classes from the training data. Ideally, we would like to minimize the variance of a finite population of size  $N_s$ :

$$\text{Var}_{N_s} = \frac{1}{N_s} \sum_{l=1}^{N_s} (\text{AUC}(S_l, g; d) - \overline{\text{AUC}}(g; d))^2.$$

Instead, in Algorithm 1, at each iteration  $t$  we sample  $n$  subsets  $S_1^{(t)}, \dots, S_n^{(t)}$  and compute

$$\widehat{\text{Var}}_n^{(t)} = \frac{N_s - n}{N_s - 1} \sum_{l=1}^n (\text{AUC}(S_l^{(t)}, g; d) - \overline{\text{AUC}}^{(t)}(g; d))^2.$$

Note that the  $n$  class subsets are drawn iid from the finite population and therefore  $\widehat{\text{Var}}_n^{(t)}$  is an unbiased <sup>1</sup> estimator of  $\text{Var}_{N_s}$ . Consequently, this procedure can be viewed as stochastic-gradient descent optimization of the objective  $\text{Var}_{N_s}$ .

**5 RESULTS**

In all experiments we compared the performance of our approach with ERM, and an adaptation of

<sup>1</sup>Due to the finite sample correction  $\frac{N_s-n}{N_s-1}$ .

**Algorithm 1: Robust Zero-Shot Representation**

**Input** : Labeled data  $D = \{z_i, c_i\}_{i=1}^{N_z}$ , number of class subsets  $n$ , number of classes within subset  $k$ , number of pairs per class  $2r$ , neural network  $g(\cdot; \theta)$ , loss  $\ell$ , distance function  $d$ , initial network weights  $\theta_0$ , number of training iterations  $T$ , learning rate  $\eta$

**Output:** Learned representation  $g(\cdot; \theta_T)$

Compute unique classes  $C^* = \{c^{(1)}, \dots, c^{(N_c)}\}$

**for**  $t = 1, \dots, T$  **do**

**for**  $l = 1, \dots, n$  **do**

        Sample  $k$  classes from  $C^*$  without replacement:  $S_l^{(t)} = \{c_l^{(1)}, \dots, c_l^{(k)}\}$

        From each class in  $S_l^{(t)}$  sample  $r$  positive and  $r$  negative training pairs. Denote the united set by  $D_l^{(t)}$ .

        Compute  $\widehat{\text{AUC}}(S_l^{(t)}, g; d)$

        Compute the average unpenalized loss over  $(x_m, y_m) \in D_l^{(t)}$ :

$$\bar{\ell}_l^{(t)} = \frac{1}{2rk} \sum_{m=1}^{2rk} \ell(x_m, y_m)$$

**end**

    Compute

$$\begin{aligned} R_{\text{VarAUC}}^{(t)} & \left( S_1^{(t)}, \dots, S_n^{(t)} \right) \\ & = \widehat{\text{Var}} \left( \widehat{\text{AUC}}(S_1^{(t)}, g; d), \dots, \widehat{\text{AUC}}(S_n^{(t)}, g; d) \right) \end{aligned}$$

    Update network parameters performing a gradient descent step:

$$\begin{aligned} \theta^{(t)} & \leftarrow \theta^{(t-1)} \\ & - \eta \nabla_{\theta} \left( \frac{1}{n} \sum_{l=1}^n \bar{\ell}_l^{(t)} + R_{\text{VarAUC}}^{(t)}(S_1^{(t)}, \dots, S_n^{(t)}) \right) \end{aligned}$$

**end**

Return  $g(\cdot; \theta_T)$

Algorithm 1 to use the IRM, CLOvE and VarREx penalties. In addition, we investigated standard regularization techniques such as dropout and the  $L_2$  norm. As anticipated, these methods led to some enhancements in the in-distribution scenario, but did not yield notable improvements in the distribution shift scenario, and therefore are not shown.

Across all experiments we used contrastive loss and normalized cosine distance:

$$d_g(z_1, z_2) = \frac{1}{2} \left( 1 - \frac{g(z_1) \cdot g(z_2)}{\|g(z_1)\| \|g(z_2)\|} \right). \quad (19)$$

Table 1: Simulation results. For each mixture ratio we report the mean AUC and (in brackets) the standard deviation across 10 repetitions of the experiment. Results are reported for in-distribution scenario ( $P_C$ ), and class distribution shift ( $Q_C$ ). Best result is marked in bold.

		In-Distribution	Distribution Shift
$\rho = 0.95$	ERM	0.955 (0.004)	0.738 (0.008)
	IRM	<b>0.956</b> (0.001)	0.740 (0.013)
	CLOvE	0.938 (0.002)	0.751 (0.015)
	VarREx	0.954 (0.005)	0.815 (0.003)
	VarAUC	0.954 (0.002)	<b>0.833</b> (0.007)
$\rho = 0.9$	ERM	<b>0.958</b> (0.004)	0.797 (0.001)
	IRM	0.944 (0.003)	0.778 (0.003)
	CLOvE	0.940 (0.005)	0.786 (0.002)
	VarREx	0.953 (0.004)	0.856 (0.008)
	VarAUC	0.950 (0.003)	<b>0.873</b> (0.013)
$\rho = 0.7$	ERM	<b>0.932</b> (0.003)	0.902 (0.002)
	IRM	0.886 (0.004)	0.850 (0.005)
	CLOvE	0.910 (0.001)	0.876 (0.005)
	VarREx	0.928 (0.002)	<b>0.911</b> (0.002)
	VarAUC	0.915 (0.002)	0.899 (0.004)

Additional details and code are provided in Section C in the supplementary material.

### 5.1 Simulations

In this section we revisit the model presented in Section 2. To elevate the complexity of the problem we add dimensions where classes from both types are not well separated. That is,  $\Sigma_z$  includes additional dimensions set practically to 0. We set  $\nu_0 = 1$ ,  $\nu^+ = 2$ ,  $\nu^- = 0.1$ . For each class  $c$  we sample 30 data points  $z_i \in \mathbb{R}^{50}$  from the distribution  $P_{Z|C}(z|c) = \mathcal{N}(c, \Sigma_z)$ . Here  $\Sigma_z$  is a diagonal matrix with 25 entries of 1 (signal dimensions) and 25 entries of 10 (noise dimensions). In each training iteration we used 68 subsets (corresponding to  $\alpha = 0.5$  and  $\rho = 0.9$ ) of two classes each, and  $2r = 10$  pairs of data points were sampled for each class. The representation was set to be  $g(z) = wz$  where  $w \in \mathbb{R}^{d \times p}$ , and  $p = 16$  is the embedding dimension. The simple representation is chosen to facilitate an analysis of the learned representation space.

Table 1 presents average AUC values for different intensities of distribution shifts (mixture proportions  $\rho$ ). The results indicate substantial improvements in robustness against class distribution shifts, especially in cases of severe shifts ( $\rho = 0.95$  and  $\rho = 0.9$ ), when utilizing our proposed framework with variance-based penalties. VarAUC penalty shows additional improvement compared to VarREx, which outperforms all other studied methods.

In Figure 2, the learning progress is depicted for  $\rho =$

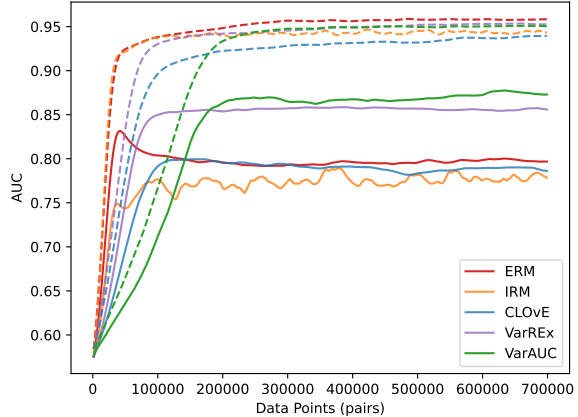


Figure 2: Average AUC progress over 10 repetitions of the simulation with  $\rho = 0.9$ . Solid lines correspond to performance on evaluation data (distribution shift scenario), dashed lines show performance on data sampled from the same distribution as training data (in-distribution scenario).

0.9. All methods perform well on data sampled from the same distribution as the training data. However, under distribution shift, the two variance-based methods show significantly better results compared to other approaches. The implementation of our algorithm with the VarREx penalty achieves high AUC values more quickly than the VarAUC penalty, but VarAUC attains higher accuracy overall. The other methods are more susceptible to distribution shifts. IRM shows noisy convergence since it is applied directly on the gradients, and these have been shown to be noisy in zero-shot learning due to high variance in data pair samples (Musgrave et al., 2020). Similar analysis for  $\rho = 0.95$  and  $\rho = 0.7$  can be found in Section A in the supplementary material.

In Figure 3 we examine the learned representation space. In our simulations, the features in the first 5 dimensions offer relatively good separation for both  $a_1$  and  $a_2$  classes (equivalent to *invariant* features in the OOD terminology). Features in dimensions 5-15 and 15-25 provide good separation for one type but not the other. Therefore, for robustness against class distribution shifts, the representation should prioritize the first 5 dimensions and treat dimensions 5-15 and 15-25 similarly. To assess the importance the representation assigns to each dimension, we calculate the absolute value of each weight relative to the others:

$$\text{Importance}_i = \left| \frac{\sum_{j=1}^p w_{ij}}{\sum_{i'=1}^d \sum_{j'=1}^p w_{i'j'}} \right|. \quad (20)$$

This analysis shows that ERM assigns the highest weights to dimensions corresponding to  $a_1$  (5-15), which is the dominant type in training. ERM assigns low weights to dimensions beneficial for both types

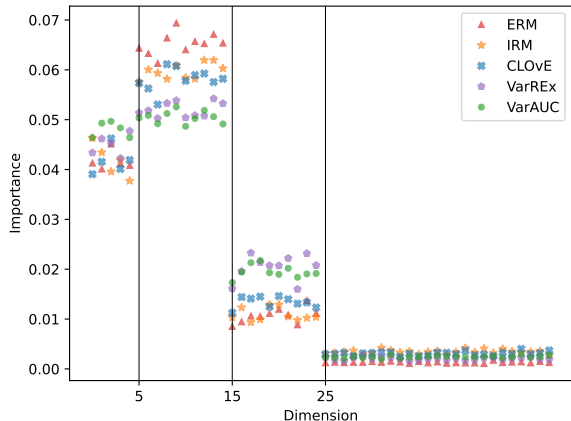


Figure 3: Feature importance results for  $\rho = 0.9$ . Reported values are average importance values over 10 repetitions.

(0-5) and those suitable for  $a_2$ . In contrast, the two variance-based methods assign the lowest weights to dimensions corresponding to  $a_1$ . They assign higher weights to shared dimensions and to those that separate well  $a_2$  classes. CLOvE and IRM assign values between ERM and the variance-based methods. The advantage VarAUC has over VarREx can be explained by VarAUC assigning more weight to dimensions corresponding to shared dimensions.

## 5.2 Experiments

Here we present the results of two experiments performed on real-world dataset for face recognition, and species recognition tasks.

**Experiment 1 - Face Recognition** We used the *CelebA* dataset (Liu et al., 2015) that contains 202,599 images of 10,177 celebrities. We filtered out people for who less than 3 images were present. Following Vinyals et al. (2016) we implemented  $g$  as a convolutional neural network which has 4 modules with a  $3 \times 3$  convolutions and 64 filters, followed by batch normalization, a ReLU activation,  $2 \times 2$  max-pooling and a fully connected layer of size 32.

We used the attribute *blond hair* for the class distribution shift: for training we sampled mostly non-blond people (95%) while in evaluation most people (95%) were blond. In each training iteration we used 150 class subsets of 2 classes each, and sampled  $2r = 20$  data points for each class.

**Experiment 2 - Species Recognition** We used the ETHEC dataset (Dhall, 2019) which includes 47,978 butterfly images from 6 families and 561 species (example images are provided in Section A in the supplementary material). We filtered out species with

Table 2: Experimental results. Mean and (in brackets) standard deviation of AUC values over 5 repetitions are reported for in distribution scenario ( $P_C(c)$ ), and class distribution shift ( $Q_C(c)$ ). Best result is marked in bold.

		In-Distribution	Distribution Shift
CelebA	ERM	0.846 (0.002)	0.678 (0.001)
	IRM	0.857 (0.011)	0.687 (0.021)
	<b>CLOvE</b>	<b>0.871</b> (0.001)	0.686 (0.015)
	VarREx	0.853 (0.003)	0.680 (0.010)
	<b>VarAUC</b>	0.863 (0.000)	<b>0.702</b> (0.002)
ETHEC	ERM	0.870 (0.003)	0.787 (0.025)
	IRM	0.883 (0.054)	0.791 (0.024)
	<b>CLOvE</b>	0.904 (0.004)	0.806 (0.021)
	<b>VarREx</b>	<b>0.928</b> (0.037)	0.807 (0.025)
	VarAUC	0.881 (0.038)	<b>0.842</b> (0.060)

less than 5 images and focused on images of butterflies from the Lycaenidae and Nymphalidae families. We included in the training set 10% of species from the Nymphalidae family, while at evaluation time 90% of the species were from the Nymphalidae family. For each class we sampled  $2r = 20$  pairs.

We trained the models on 200 class subsets at a time, each of two classes. We implemented  $g$  as a fully connected neural network with layers of sizes 128, 64, 32 and 16, and ReLU activations between them.

The results, summarized in Table 2, show that all penalized methods achieve some improvement on the in-distribution setting, especially the VarREx penalty. Under distribution shift VarAUC achieves best results, outperforming VarREx even by a larger margin compared to simulations. Section A of the supplementary material provides additional analysis.

## 6 Conclusion

In this work we introduced a novel framework to investigate class distribution shifts caused by changes in unknown underlying attributes in zero-shot learning. We showed that by defining environments using hierarchical sampling, OOD methods can be applied to improve robustness with respect to class distribution shifts. Additionally, we proposed a penalty term specifically designed for balancing performance across data subsets for algorithms trained using deep metric learning losses. While our focus was on verification zero-shot classifiers, its importance extends beyond these algorithms. First, a similar framework could be explored in closed-world classification to enhance robustness against shifts in an unknown attribute. Second, the penalty we introduced holds potential for broader applications in the realm of out-of-distribution generalization. These extensions are promising directions for future work.

## References

- Martin Arjovsky, Léon Bottou, Ishaan Gulrajani, and David Lopez-Paz. Invariant risk minimization. *arXiv preprint arXiv:1907.02893*, 2019.
- Aharon Ben-Tal, Dick Den Hertog, Anja De Waegenare, Bertrand Melenberg, and Gijs Rennen. Robust solutions of optimization problems affected by uncertain probabilities. *Management Science*, 59(2):341–357, 2013.
- Lacey Best-Rowden and Anil K Jain. Longitudinal study of automatic face recognition. *IEEE transactions on pattern analysis and machine intelligence*, 40(1):148–162, 2017.
- Jonathon Byrd and Zachary Lipton. What is the effect of importance weighting in deep learning? In *International conference on machine learning*, pages 872–881. PMLR, 2019.
- Toon Calders and Szymon Jaroszewicz. Efficient auc optimization for classification. In *European conference on principles of data mining and knowledge discovery*, pages 42–53. Springer, 2007.
- Kaidi Cao, Colin Wei, Adrien Gaidon, Nikos Arechiga, and Tengyu Ma. Learning imbalanced datasets with label-distribution-aware margin loss. *Advances in neural information processing systems*, 32, 2019.
- Shiyu Chang, Yang Zhang, Mo Yu, and Tommi Jaakkola. Invariant rationalization. In *International Conference on Machine Learning*, pages 1448–1458. PMLR, 2020.
- Yin Cui, Menglin Jia, Tsung-Yi Lin, Yang Song, and Serge Belongie. Class-balanced loss based on effective number of samples. In *Proceedings of the IEEE/CVF conference on computer vision and pattern recognition*, pages 9268–9277, 2019.
- Ankit Dhall. Eth entomological collection (ethec) dataset [paleartic macrolepidoptera, spring 2019]. 2019.
- John C Duchi and Hongseok Namkoong. Learning models with uniform performance via distributionally robust optimization. *The Annals of Statistics*, 49(3):1378–1406, 2021.
- John C Duchi, Peter W Glynn, and Hongseok Namkoong. Statistics of robust optimization: A generalized empirical likelihood approach. *Mathematics of Operations Research*, 46(3):946–969, 2021.
- Li Fei-Fei, Rob Fergus, and Pietro Perona. One-shot learning of object categories. *IEEE transactions on pattern analysis and machine intelligence*, 28(4):594–611, 2006.
- Patrick Grother, Mei Ngan, Kayee Hanaoka, et al. Ongoing face recognition vendor test (frvt) part 3: Demographic effects. *Nat. Inst. Stand. Technol., Gaithersburg, MA, USA, Rep. NISTIR*, 8280, 2019.
- Zhangxuan Gu, Siyuan Zhou, Li Niu, Zihan Zhao, and Liqing Zhang. Context-aware feature generation for zero-shot semantic segmentation. In *Proceedings of the 28th ACM International Conference on Multimedia*, pages 1921–1929, 2020.
- Raia Hadsell, Sumit Chopra, and Yann LeCun. Dimensionality reduction by learning an invariant mapping. In *2006 IEEE Computer Society Conference on Computer Vision and Pattern Recognition (CVPR'06)*, volume 2, pages 1735–1742. IEEE, 2006.
- Alexander Hermans, Lucas Beyer, and Bastian Leibe. In defense of the triplet loss for person re-identification. *arXiv preprint arXiv:1703.07737*, 2017a.
- Alexander Hermans, Lucas Beyer, and Bastian Leibe. In defense of the triplet loss for person re-identification. *arXiv preprint arXiv:1703.07737*, 2017b.
- Elad Hoffer and Nir Ailon. Deep metric learning using triplet network. In *International workshop on similarity-based pattern recognition*, pages 84–92. Springer, 2015.
- Badr Youbi Idrissi, Martin Arjovsky, Mohammad Pezeshki, and David Lopez-Paz. Simple data balancing achieves competitive worst-group-accuracy. In *Conference on Causal Learning and Reasoning*, pages 336–351. PMLR, 2022.
- Aparna R Joshi, Xavier Suau Cuadros, Nivedha Sivakumar, Luca Zappella, and Nicholas Apostoloff. Fair sa: Sensitivity analysis for fairness in face recognition. In *Algorithmic fairness through the lens of causality and robustness workshop*, pages 40–58. PMLR, 2022.
- Brendan F Klare, Mark J Burge, Joshua C Klontz, Richard W Vorder Bruegge, and Anil K Jain. Face recognition performance: Role of demographic information. *IEEE Transactions on information forensics and security*, 7(6):1789–1801, 2012.
- Gregory Koch, Richard Zemel, Ruslan Salakhutdinov, et al. Siamese neural networks

- for one-shot image recognition. In *International Conference on Machine Learning (ICML) deep learning workshop*, volume 2, 2015.
- David Krueger, Ethan Caballero, Joern-Henrik Jacobsen, Amy Zhang, Jonathan Binas, Dinghui Zhang, Remi Le Priol, and Aaron Courville. Out-of-distribution generalization via risk extrapolation (rex). In *International Conference on Machine Learning*, pages 5815–5826. PMLR, 2021.
- Aviral Kumar, Sunita Sarawagi, and Ujjwal Jain. Trainable calibration measures for neural networks from kernel mean embeddings. In Jennifer Dy and Andreas Krause, editors, *Proceedings of the 35th International Conference on Machine Learning*, volume 80 of *Proceedings of Machine Learning Research*, pages 2805–2814. PMLR, 10–15 Jul 2018. URL <https://proceedings.mlr.press/v80/kumar18a.html>.
- Hugo Larochelle, Dumitru Erhan, and Yoshua Bengio. Zero-data learning of new tasks. In *AAAI*, volume 1, page 3, 2008.
- Tsung-Yi Lin, Priya Goyal, Ross Girshick, Kaiming He, and Piotr Dollár. Focal loss for dense object detection. In *Proceedings of the IEEE international conference on computer vision*, pages 2980–2988, 2017.
- Evan Z Liu, Behzad Haghgoo, Annie S Chen, Aditi Raghunathan, Pang Wei Koh, Shiori Sagawa, Percy Liang, and Chelsea Finn. Just train twice: Improving group robustness without training group information. In *International Conference on Machine Learning*, pages 6781–6792. PMLR, 2021.
- Ziwei Liu, Ping Luo, Xiaogang Wang, and Xiaoou Tang. Deep learning face attributes in the wild. In *Proceedings of International Conference on Computer Vision (ICCV)*, December 2015.
- Nicolai Meinshausen and Peter Bühlmann. Maximin effects in inhomogeneous large-scale data. *The Annals of Statistics*, pages 1801–1830, 2015.
- Aditya Krishna Menon, Sadeep Jayasumana, Ankit Singh Rawat, Himanshu Jain, Andreas Veit, and Sanjiv Kumar. Long-tail learning via logit adjustment. In *International Conference on Learning Representations*, 2020.
- Dana Michalski, Sau Yee Yiu, and Chris Malec. The impact of age and threshold variation on facial recognition algorithm performance using images of children. In *2018 International Conference on Biometrics (ICB)*, pages 217–224. IEEE, 2018.
- Kevin Musgrave, Serge Belongie, and Ser-Nam Lim. A metric learning reality check. In *Computer Vision—ECCV 2020: 16th European Conference, Glasgow, UK, August 23–28, 2020, Proceedings, Part XXV 16*, pages 681–699. Springer, 2020.
- Hyun Oh Song, Yu Xiang, Stefanie Jegelka, and Silvio Savarese. Deep metric learning via lifted structured feature embedding. In *Proceedings of the IEEE conference on computer vision and pattern recognition*, pages 4004–4012, 2016.
- Jonas Peters, Peter Bühlmann, and Nicolai Meinshausen. Causal inference by using invariant prediction: identification and confidence intervals. *Journal of the Royal Statistical Society Series B: Statistical Methodology*, 78(5):947–1012, 2016.
- Jonas Peters, Dominik Janzing, and Bernhard Schölkopf. *Elements of causal inference: foundations and learning algorithms*. The MIT Press, 2017.
- Vihari Piratla, Praneeth Netrapalli, and Sunita Sarawagi. Focus on the common good: Group distributional robustness follows. In *International Conference on Learning Representations*, 2021.
- Inioluwa Deborah Raji and Joy Buolamwini. Actionable auditing: Investigating the impact of publicly naming biased performance results of commercial ai products. In *Proceedings of the 2019 AAAI/ACM Conference on AI, Ethics, and Society*, pages 429–435, 2019.
- Jiawei Ren, Cunjun Yu, Xiao Ma, Haiyu Zhao, Shuai Yi, et al. Balanced meta-softmax for long-tailed visual recognition. *Advances in neural information processing systems*, 33:4175–4186, 2020.
- Joseph P Robinson, Gennady Livitz, Yann Henon, Can Qin, Yun Fu, and Samson Timoner. Face recognition: too bias, or not too bias? In *Proceedings of the IEEE/CVF Conference on Computer Vision and Pattern Recognition Workshops*, pages 0–1, 2020.
- Mateo Rojas-Carulla, Bernhard Schölkopf, Richard Turner, and Jonas Peters. Invariant models for causal transfer learning. *The Journal of Machine Learning Research*, 19(1):1309–1342, 2018.
- Karsten Roth, Timo Milbich, Samarth Sinha, Prateek Gupta, Bjorn Ommer, and Joseph Paul Cohen. Revisiting training strategies and generalization performance in deep metric learning. In *International Conference on Machine Learning*, pages 8242–8252. PMLR, 2020.
- Dominik Rothenhäusler, Nicolai Meinshausen, Peter Bühlmann, and Jonas Peters. Anchor regression:

- Heterogeneous data meet causality. *Journal of the Royal Statistical Society Series B: Statistical Methodology*, 83(2):215–246, 2021.
- Marco Saerens, Patrice Latinne, and Christine Decaestecker. Adjusting the outputs of a classifier to new a priori probabilities: a simple procedure. *Neural computation*, 14(1):21–41, 2002.
- Shiori Sagawa, Pang Wei Koh, Tatsunori B Hashimoto, and Percy Liang. Distributionally robust neural networks. In *International Conference on Learning Representations*, 2019.
- Hidetoshi Shimodaira. Improving predictive inference under covariate shift by weighting the log-likelihood function. *Journal of statistical planning and inference*, 90(2):227–244, 2000.
- Tomáš Sixta, Julio CS Jacques Junior, Pau Buch-Cardona, Eduard Vazquez, and Sergio Escalera. Fairface challenge at eccv 2020: Analyzing bias in face recognition. In *Computer Vision—ECCV 2020 Workshops: Glasgow, UK, August 23–28, 2020, Proceedings, Part VI 16*, pages 463–481. Springer, 2020.
- Yuli Slavutsky and Yuval Benjamini. Predicting classification accuracy when adding new unobserved classes. In *International Conference on Learning Representations, ICLR, Conference Track Proceedings*, 2021.
- Kihyuk Sohn. Improved deep metric learning with multi-class n-pair loss objective. *Advances in neural information processing systems*, 29, 2016.
- Nisha Srinivas, Karl Ricanek, Dana Michalski, David S Bolme, and Michael King. Face recognition algorithm bias: Performance differences on images of children and adults. In *Proceedings of the IEEE/CVF conference on computer vision and pattern recognition workshops*, pages 0–0, 2019.
- Oriol Vinyals, Charles Blundell, Timothy Lillicrap, Daan Wierstra, et al. Matching networks for one shot learning. *Advances in neural information processing systems*, 29, 2016.
- Yoav Wald, Amir Feder, Daniel Greenfeld, and Uri Shalit. On calibration and out-of-domain generalization. *Advances in neural information processing systems*, 34:2215–2227, 2021.
- Mei Wang and Weihong Deng. Mitigating bias in face recognition using skewness-aware reinforcement learning. In *Proceedings of the IEEE/CVF conference on computer vision and pattern recognition*, pages 9322–9331, 2020.
- Mei Wang, Weihong Deng, Jiani Hu, Xunqiang Tao, and Yaohai Huang. Racial faces in the wild: Reducing racial bias by information maximization adaptation network. In *Proceedings of the IEEE/cvf international conference on computer vision*, pages 692–702, 2019.
- Jiaheng Wei, Harikrishna Narasimhan, Ehsan Amid, Wen-Sheng Chu, Yang Liu, and Abhishek Kumar. Distributionally robust post-hoc classifiers under prior shifts. In *International Conference on Learning Representations (ICLR)*, 2023.
- Chao-Yuan Wu, R Manmatha, Alexander J Smola, and Philipp Krahenbuhl. Sampling matters in deep embedding learning. In *Proceedings of the IEEE international conference on computer vision*, pages 2840–2848, 2017.
- Yongqin Xian, Subhabrata Choudhury, Yang He, Bernt Schiele, and Zeynep Akata. Semantic projection network for zero-and few-label semantic segmentation. In *Proceedings of the IEEE/CVF Conference on Computer Vision and Pattern Recognition*, pages 8256–8265, 2019.
- Tongtong Yuan, Weihong Deng, Jian Tang, Yinan Tang, and Binghui Chen. Signal-to-noise ratio: A robust distance metric for deep metric learning. In *Proceedings of the IEEE/CVF conference on computer vision and pattern recognition*, pages 4815–4824, 2019.
- Charles Zheng, Rakesh Achanta, and Yuval Benjamini. Extrapolating expected accuracies for large multi-class problems. *The Journal of Machine Learning Research*, 19(1):2609–2638, 2018.
- Zhisheng Zhong, Jiequan Cui, Shu Liu, and Jiaya Jia. Improving calibration for long-tailed recognition. In *Proceedings of the IEEE/CVF conference on computer vision and pattern recognition*, pages 16489–16498, 2021.

## A ADDITIONAL RESULTS

### A.1 Additional Simulation Results

AUC progress during training iterations and feature importance results for the majority class proportion of  $\rho = 0.9$  were shown in the main text. Here, we provide analogous results for  $\rho = 0.95$  and  $\rho = 0.7$ . These are summarized in Figure 4.

For  $\rho = 0.95$  the convergence results are similar to those obtained for  $\rho = 0.9$  – under distribution-shift the two variance based methods show significantly better results compared to other approaches. Our algorithm with the VarREx penalty achieves high AUC values more quickly than the VarAUC penalty, but the VarAUC penalty attains higher accuracy overall. The CLOvE penalty achieves improvement over ERM, but smaller compared to the variance based methods. IRM converges to the same AUC as ERM. In contrast, on in-distribution data all methods perform well.

For  $\rho = 0.7$  the distribution shift is milder and therefore ERM performs very well (0.902 AUC is achieved on distribution shift scenario compared to 0.932 on in-distribution setting). Therefore encouragement of similar performance across different data subsets does not benefit the learning process. Slightly better result is achieved with VarREx penalty (0.911).

The analysis of feature importance for  $\rho = 0.95$  yields results similar to those for  $\rho = 0.9$ . At  $\rho = 0.7$  the analysis remains mostly unchanged, except that VarREx assigns higher importance to features corresponding to  $\nu_0$  (0-5) compared to VarAUC, while in more extreme distribution shifts VarAUC assigns higher importance to the shared features.

### A.2 Analysis of Loss Values

Here we present an analysis of the unpenalized loss after convergence in both real-data experiments. We performed separate analyses on pairs of data points from the dominant type during training (majority), and those from the other type (minority). Additionally, we separated positive pairs ( $y = 1$ ) and negative pairs ( $y = 0$ ). Figure 5 displays histograms illustrating the differences between losses on the training set obtained with the representation learned using ERM ( $g_{\text{ERM}}$ ), and those obtained using our algorithm with VarAUC penalty ( $g_{\text{VarAUC}}$ ):

$$\text{Diff}_{ij} = \ell(x_{ij}, y_{ij}; d_{g_{\text{ERM}}}) - \ell(x_{ij}, y_{ij}; d_{g_{\text{VarAUC}}}).$$

Positive values of the differences correspond to higher losses for ERM.

In both experiments, when examining negative pairs from the minority group, as shown in the top-left histograms, most of the observed differences are positive. This indicates that the ERM losses for these pairs are higher compared to the losses obtained for the representation trained with the VarAUC penalty. The disparities are smaller for the other three groups: majority negative pairs, minority negative pairs, and minority positive pairs. Among these groups, ERM performs better on positive pairs.

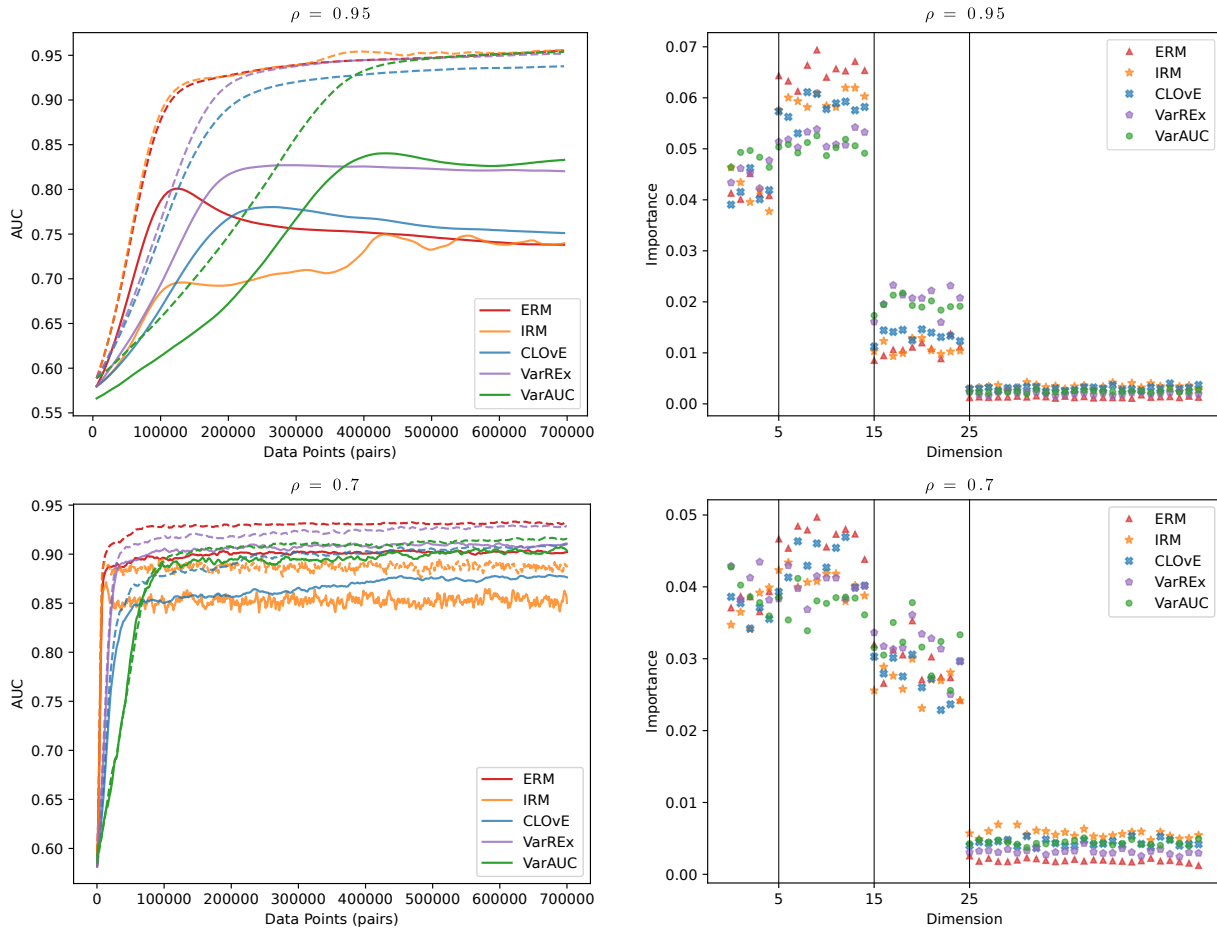


Figure 4: Additional Simulation Results. Top row:  $\rho = 0.95$ , Bottom row:  $\rho = 0.7$ . Left: Average AUC progress over 10 repetitions of the simulation. Solid lines correspond to performance on evaluation data (distribution shift scenario), dashed lines show performance on data sampled from the same distribution as training data (in-distribution scenario). Right: Average feature importance results over 10 repetitions.

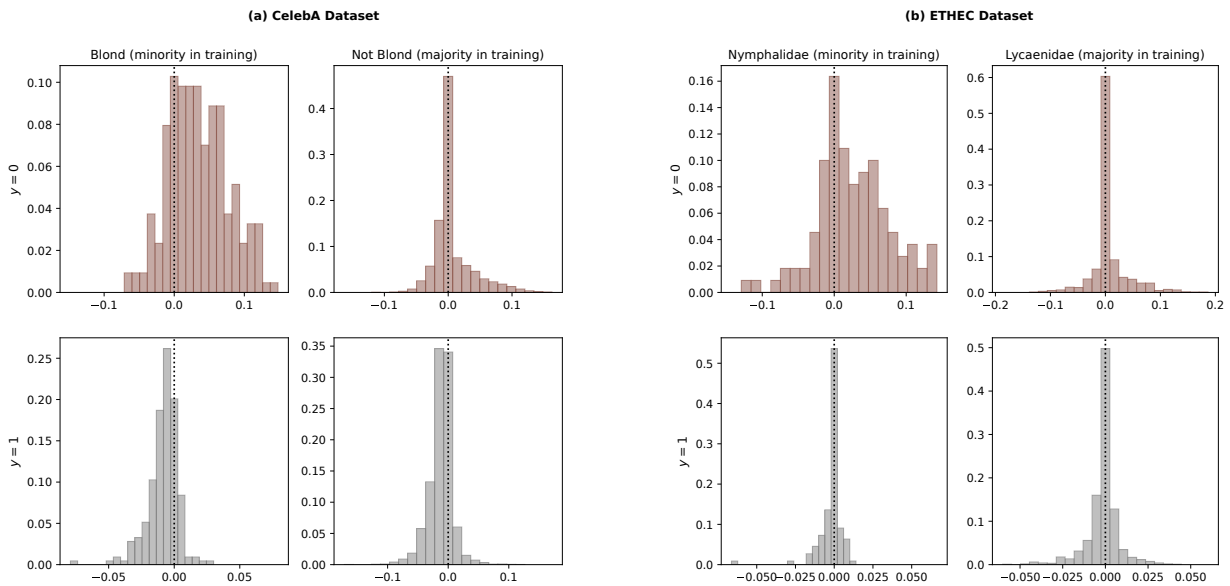


Figure 5: Analysis of Loss Differences. Histograms of differences between ERM and our algorithm with VarAUC penalty are shown for two experiments in separate sub-figures: (a) CelebA dataset, (b) ETHEC dataset. The top rows show differences for negative pairs ( $y = 0$ ), bottom ones show differences for positive pairs ( $y = 1$ ). In each sub-figure the left column corresponds to the minority type and right one to the majority. A dotted black line marks a difference of 0. Positive values correspond to higher losses for ERM.

## B Datasets



Figure 6: Sample Images from the CelebA Dataset. Top: a random sample of the training data with 95% non-blond people. Bottom: a random sample of the test data with 95% blond people.

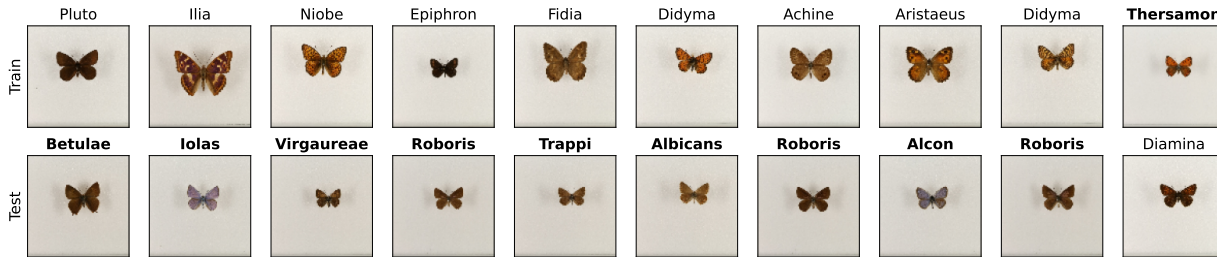


Figure 7: Sample Images from the ETHEC Dataset. Top: a sample of the the training data – 9 species of the Lycaenidae family and 1 from the Nymphalidae family. Bottom: a sample of the test data where the proportion of the families is reversed. Nymphalidae species names are marked in bold.

## C IMPLEMENTATION DETAILS

Code to reproduce our results is attached to the submission and upon acceptance a link to a permanent repository will be included in the main text.

The data-related parameters of our experiments are described in the main text. In all our experiments we used margin of  $m = 0.5$  for the contrastive loss and Adam (Kingma & Ba, 2014) optimizer to train all models.

For the CLOvE penalty we used a Laplacian kernel  $k(r, r') = e^{-\frac{1}{\text{width}}|r-r'|}$  with width of 0.4 as originally suggested by Kumar et al. (2018).

For optimization of the VarAUC objective we disregard the finite sample correction  $\frac{N_s-n}{N_s-1}$  in the implementation since  $n$  is very small compared to  $N_s$ . In practice, we minimize the standard deviation instead of the variance in both variance based penalties, and the hyperparameters are reported accordingly.

Hyper-parameters for all methods were selected through grid-search on one excluded experiment repetition. For the simulations  $\rho = 0.9$  was used to perform the grid search. We observed minimal differences in optimal learning rates among the methods within an experiment. Therefore, for simplicity, we used a shared learning rate for each experiment, optimized for the ERM method. The chosen hyper-parameters are listed in Table 3.

All models were initialized with identical weights, and trained on identically ordered data.

All the code in this work was implemented in Python 3.10. We used the TensorFlow 2.13 and TensorFlow Addons 0.21 packages. For evaluation we used the auc function from scikit-learn 1.2. The CelebA dataset was loaded through TensorFlow Datasets 4.9 and pandas 1.5 was used to process the ETHEC dataset. All figures were generated using Matplotlib 3.7. We ran all experiments on A100 cloud GPUs.

The IRM implementation was adapted from the source code of the paper, available at <https://github.com/facebookresearch/InvariantRiskMinimization>.

Table 3: Hyper Parameters.

		ERM	IRM	CLOvE	VarREx	VarAUC
Simulations	Learning rate $\eta$	0.01	0.01	0.01	0.01	0.01
	Regularization factor $\lambda$	–	0.01	0.085	3.0	1.3
	Network weight regularizer	–	0.01	–	–	–
CelebA	Learning rate $\eta$	$10^{-5}$	$10^{-5}$	$10^{-5}$	$10^{-5}$	$10^{-5}$
	Regularization factor $\lambda$	–	0.1	0.085	0.01	0.2
	Network weight regularizer	–	0.01	–	–	–
ETHEC	Learning rate $\eta$	$10^{-3}$	$10^{-3}$	$10^{-3}$	$10^{-3}$	$10^{-3}$
	Regularization factor $\lambda$	–	0.02	0.05	0.1	0.2
	Network weight regularizer	–	0.01	–	–	–